Inorg. Chem. **2003**, *42*, 8439–8445

Equilibrium Studies in Solution Involving Nickel(II) Complexes of Flexidentate Schiff Base Ligands: Isolation and Structural Characterization of the Planar Red and Octahedral Green Species Involved in the Equilibrium

Suman Mukhopadhyay,[†] Debdas Mandal,[†] Dipesh Ghosh,[†,§] Israel Goldberg,[‡] and Muktimoy Chaudhury*[,†]

Department of Inorganic Chemistry, Indian Association for the Cultivation of Science, Kolkata 700 032, India, and School of Chemistry, Tel Aviv University, Tel Aviv 69978, Israel

Received June 4, 2003

Three new flexidentate 5-substituted salicylaldimino Schiff base ligands (L^1-OH–L^3-OH) based on 1-(2-aminoethyl)-piperazine (X = H, L^1-OH; X = NO_2, L^2-OH; and X = Br, L^3-OH) and their nickel(II) complexes (**1a**, **1b**, **2**, and **3**) have been reported. The piperazinyl arm of these ligands can in principle have both boat and chair conformations that allow the ligands to bind the Ni(II) center in an ambidentate manner, forming square-planar and/or octahedral complexes. The nature of substitution in the salicylaldehyde aromatic ring and the type of associated anion in the complexes have profound influences on the coordination geometry of the isolated products. With the parent ligand L^1-OH, the product obtained is either a planar red compound $[Ni(L^1\text{-}O)]^+$, isolated as tetraphenylborate salt (**1a**), or an octahedral green compound $[Ni(L^1\text{-}NH)(H_2O)_3]^{2+}$, isolated with sulfate anion (**1b**); both have been crystallographically characterized. In aqueous solution, both these planar ($S = 0$) and octahedral ($S = 1$) forms are in equilibrium that has been followed in the temperature range 298–338 K by ^{1}H NMR technique using the protocol of Evans's method. The large exothermicity of the equilibrium process $[Ni(L^1\text{-}O)]^+ + 3H_2O + H^+ \rightleftharpoons [Ni(L^1\text{-}NH)(H_2O)_3]^{2+}$ ($\Delta H° = -46 \pm 0.2$ kJ mol^{-1} and $\Delta S° = -133 \pm 5$ J K^{-1} mol^{-1}) reflects formation of three new Ni–OH_2 bonds in going from planar to the octahedral species. With the 5-nitro derivative ligand L^2-OH, the sole product is an octahedral compound **2**, isolated as a sulfate salt while with the bromo derivative ligand L^3-OH, the exclusive product is a planar molecule **3** with associated tetraphenylborate anion. Both **2** and **3** have been structurally characterized by X-ray diffraction analysis.

Introduction

The possibility of the existence of an equilibrium in solution between the octahedral and planar forms of nickel(II) complexes was reported for the first time with some sterically constrained ligands, viz. stilbenediamine (stien) by Lifschitz et al.[1,2] The proposed equilibrium $[Ni(stein)X_2] \rightleftharpoons [Ni(stien)^{2+}] + 2X^-$ (X^- = various anions) was latter established by magnetic, spectroscopic, and X-ray structure analyses.[3,4] Over the years, several other such equilibria have been reported using macrocyclic[5−12] and open chain

* Author to whom correspondence should be addressed. E-mail: icmc@mahendra.iacs.res.in.
† Indian Association for the Cultivation of Science.
‡ Tel Aviv University.
§ Present address: Department of Chemistry, University of Missouri—Kansas City, Kansas City, MO 64110.

(1) Lifschitz, I.; Bos, J. G.; Dijkema, K. M. *Z. Anorg. Allg. Chem.* **1939**, *24*, 97.
(2) Lifschitz, I.; Bos, J. G. *Recl. Trav. Chim.* **1940**, *5*, 407.
(3) Higginson, W. C. E.; Nyburg, S. C.; Wood, J. S. *Inorg. Chem.* **1964**, *3*, 463.
(4) Nyburg, S. C.; Wood, J. S. *Inorg. Chem.* **1964**, *3*, 468.
(5) Fabbrizzi, L.; Paoletti, P.; Clay, R. M. *Inorg. Chem.* **1978**, *17*, 1042.
(6) Sabatini, L.; Fabbrizzi, L. *Inorg. Chem.* **1979**, *18*, 438.
(7) Swisher, R. G.; Dayhuff, J. P.; Stuehr, D. J.; Blinn, E. L. *Inorg. Chem.* **1980**, *19*, 1336.
(8) Hay, R. W.; Bembi, R.; Sommerville, W. *Inorg. Chim. Acta* **1982**, *59*, 147.
(9) Steenland, M. W. A.; Dierck, I.; Herman, G. G.; Devreese, B.; Lippens, W.; Van Beeumen, J.; Goeminne, A. M. *J. Chem. Soc., Dalton Trans.* **1997**, 3637.
(10) Sakata, K.; Wada, S.; Sato, N.; Kurisu, M.; Hashimoto, M.; Kato, Y. *Inorg. Chim. Acta* **1986**, *119*, 111.
(11) Bembi, R.; Bhardwarj, V. K.; Singh, R.; Singh, R.; Taneja, K.; Aftab, S. *Inorg. Chem.* **1984**, *23*, 4153.
(12) Hay, R. W.; Jeragh, B.; Ferguson, G.; Kaitner, B.; Ruhl, B. L. *J. Chem. Soc., Dalton Trans.* **1982**, 1531.

10.1021/ic0346174 CCC: $25.00
Published on Web 11/11/2003

Scheme 1

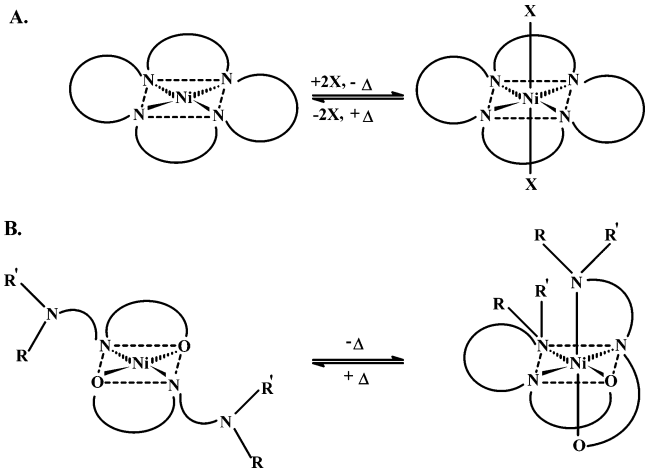

polyamines and Schiff base ligands.[13−16] These reported equilibria are generally of two types (Scheme 1). The most common one involves axial attachment of ligand X (X = anions or solvent molecules, predominantly water) to square-planar species NiL, largely of macrocyclic ligands L (Scheme 1A) to generate the octahedral counterpart $NiLX_2$.[5−14] The second type of equilibrium (Scheme 1B), on the other hand, involves flexidentate ligands (L′) which form bis complexes of composition $Ni(L')_2$. At lower temperatures, these ligands bind nickel(II) in tridentate fashion to render octahedral geometry which reduces to a planar one at elevated temperatures due to steric constraints of the associated ligands.[15,16] Most of these equilibrium studies were followed by spectroscopic techniques, and only in a few cases were the species involved characterized in the solid state by X-ray diffraction analysis.[4,12]

Recently, reports have been made on pH-dependent reversible translocation of Ni(II) ion from octahedral to the square-planar site in ditopic ligand systems.[17] Such a translocation phenomenon can be used effectively as a light emission switch by tagging the ditopic ligand systems with fluorescent probes.[18,19]

Herein, we report the nickel(II) complexes of three new flexidentate Schiff base ligands (L^1-OH−L^3-OH; Chart 1).[20] The piperazinyl arm of these ligands can, in principle, have both boat and chair conformations that force these molecules to display ambidentate ligation behavior, leading to both octahedral and square-planar geometry for the Ni(II) complexes. The structures of these complexes in the solid state have been examined by X-ray diffraction analysis. The square-planar−octahedral equilibrium in solution is followed in detail by ^{1}H NMR and electronic spectroscopies.

Chart 1

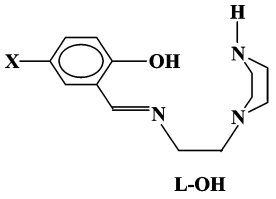

X	L-OH
H	L^1-OH
NO_2	L^2-OH
Br	L^3-OH

Experimental Section

Materials. 1-(2-Aminoethyl)piperazine, 5-bromosalicylaldehyde, and 5-nitrosalicylaldehyde were obtained from Aldrich. Salicylaldehyde (Aldrich) was distilled before use. Solvents were reagent grade, dried from appropriate reagents,[21] and distilled under nitrogen prior to their use. Spectroscopic grade D_2O was also obtained from Aldrich. All other chemicals were commercially available and used as received.

Syntheses. Ligands. The Schiff base ligands (L^1-OH−L^3-OH) were prepared following a general procedure. Synthesis of 1-(2-salicylaldiminoethyl)piperazine (L^1-OH) is described below as a prototype.

To a stirred solution of salicylaldehyde (2.44 g, 20 mmol) in absolute ethanol (20 mL) was added dropwise an equimolar amount (2.58 g) of 1-(2-aminoethyl)piperazine, and the resulting mixture was refluxed for 1 h to obtain an orange solution. The solvent was then removed by rotary evaporation to obtain a red oil which on standing for days in a vacuum produced a yellow hygroscopic solid. Several attempts to recrystallize the compound were unsuccessful.

Both ligands L^2-OH and L^3-OH are also extremely hygroscopic yellow solids, which eluded our repeated attempts at recrystallization. The ligands were then used for metalation without further purification.

Complexes. [Ni(L^1-O)](BPh$_4$) (1a). To a stirred solution of L^1-OH (0.23 g, 1 mmol) in methanol (20 mL) was added a solution of $Ni(ClO_4)_2 \cdot 6H_2O$ (0.36 g, 1 mmol) taken also in methanol. The resultant orange solution was refluxed for 2 h. Solid $NaBPh_4$ (0.50 g) was then added to the solution while it was hot and filtered immediately. The filtrate was kept in the air for ca. 12 h to obtain an orange microcrystalline solid. It was collected by filtration, washed with Et_2O (5 × 2 mL), and dried in a vacuum. The compound was recrystallized from CH_2Cl_2/*n*-hexane mixture. Diffraction quality crystals were obtained by diffusing *n*-hexane into a dichloromethane solution of the compound. Yield: 0.34 g (55%). Anal. Calcd for $C_{37}H_{38}BNiN_3O$: C, 72.76; H, 6.23; N, 6.88. Found: C, 73.03; H, 6.29; N, 6.70. IR (KBr disk, cm^{-1}): ν(N−H), 3263s; ν(C=N), 1618s; ν(C−O/phenolate), 1530s; ν(phenyl ring), 738s, 706s.

[Ni(L^1-NH)(H_2O)$_3$](SO_4)·6H_2O (1b). An aqueous solution (25 mL) of $NiSO_4 \cdot 6H_2O$ (0.26 g, 1 mmol) was added dropwise to a solution of the ligand L^1-OH (0.23 g, 1 mmol) taken in methanol (10 mL). The resultant green solution was stirred for 30 min and

(13) Anichini, A.; Fabbrizzi, L.; Paoletti, P. *Inorg. Chim. Acta* **1977**, *24*, L21.
(14) Evans, D. F.; Missen, P. H. *J. Chem. Soc., Dalton Trans.* **1985**, 1451.
(15) Sacconi, L.; Nannelli, P.; Nardi, N.; Campigli, U. *Inorg. Chem.* **1965**, *4*, 943.
(16) Sacconi, L.; Nardi, N.; Zanobini, F. *Inorg. Chem.* **1966**, *5*, 1872.
(17) Amendola, V.; Fabbrizzi, L.; Mangano, C.; Pallavicini, P. *Acc. Chem. Res.* **2001**, *34*, 488.
(18) Fabbrizzi, L.; Foti, F.; Licchelli, M.; Poggi, A. *Inorg. Chem.* **2002**, *41*, 4612.
(19) Fabbrizzi, L.; Licchelli, M.; Pallavicini, P.; Parodi, L. *Angew. Chem., Int. Ed.* **1998**, *37*, 800.
(20) In the ligand L-OH, the dissociable proton is attached to the phenolic oxygen atom. L-NH, on the other hand, represents the N (piperazine)-protonated, O (phenol)-deprotonated form of the ligand.
(21) Perin, D. D.; Armarego, W. L. F.; Perrin, D. R. *Purification of Laboratory Chemicals*, 2nd ed.; Pergamon: Oxford, England, 1980.

Table 1. Relevant Crystal Data for $[Ni(L^1\text{-}O)](BPh_4)$ (**1a**), $[Ni(L^1\text{-}NH)(H_2O)_3](SO_4)\cdot 6H_2O$ (**1b**), $[Ni(L^2\text{-}NH)(H_2O)_3](SO_4)\cdot 2H_2O$ (**2**), and $[Ni(L^3\text{-}O)](BPh_4)$ (**3**)

	1a	**1b**	**2**	**3**
empirical formula	$C_{37}H_{38}BNiN_3O$	$C_{13}H_{37}NiN_3O_{14}S$	$C_{13}H_{28}NiN_4O_{12}S$	$C_{37}H_{37}BBrNiN_3O$
formula weight	610.22	550.23	523.16	689.13
cryst size (mm^3)	0.30 × 0.30 × 0.45	0.10 × 0.10 × 0.30	0.10 × 0.15 × 0.25	0.10 × 0.10 × 0.20
cryst system	triclinic	triclinic	triclinic	hexagonal
space group	$P\bar{1}$	$P\bar{1}$	$P\bar{1}$	$P6_5$
T (K)	293	110	110	110
a (Å)	9.6549(5)	8.8690(1)	9.0570(1)	9.7290(1)
b (Å)	9.7345(5)	11.9180(2)	9.5280(1)	9.7290(1)
c (Å)	18.0363(9)	12.1220(2)	14.2900(2)	56.9660(13)
α (deg)	98.6550(10)	100.3600(6)	77.6760(9)	90.00
β (deg)	99.3440(10)	109.7881(7)	72.6110(10)	90.00
γ (deg)	110.5200(10)	93.5550(10)	64.2060(2)	120.00
V $(Å)^3$	1526.57(13)	1175.49(3)	1054.55(2)	4669.63(13)
Z	2	2	2	6
ρ_{calcd} (g cm^{-3})	1.328	1.554	1.648	1.470
F(000)	644	584	548	2136
radiation used	Mo Kα	Mo Kα	Mo Kα	Mo Kα
R_1, wR_2 (all data)	0.061, 0.102	0.036, 0.086	0.027, 0.064	0.093, 0.138
R_1, wR_2 (data with $I > 2\sigma_I$)	0.042, 0.095	0.033, 0.083	0.025, 0.062	0.057, 0.118
GOF	1.010	0.975	1.024	0.942

filtered. The filtrate was concentrated under reduced pressure to drive off methanol and filtered again. The filtrate was layered with acetone and kept at 4 °C for several days to obtain a moss-green crystalline compound along with some X-ray diffraction quality crystals. The product was collected by filtration and dried over fused $CaCl_2$. Yield: 0.14 g (25%). Anal. Calcd for $C_{13}H_{37}NiN_3O_{14}S$: C, 28.35; H, 6.72; N, 7.63. Found: C, 29.16; H, 6.71; N, 7.85. IR (KBr disk, cm^{-1}): ν(O−H), 3406b; ν(C═N), 1648s; ν(C−O)/phenolate, 1548s; $\nu(SO_4)$, 1111s and 620s. $\mu_{eff} = 3.32\ \mu_B$ at 25 °C.

$[Ni(L^2\text{-}NH)(H_2O)_3](SO_4)\cdot 2H_2O$ (2). An aqueous solution (25 mL) of $NiSO_4\cdot 6H_2O$ (0.26 g, 1 mmol) was added dropwise to a stirred solution of the ligand L^2-OH (0.28 g, 1 mmol), dissolved in methanol (10 mL). A yellow compound was precipitated almost immediately, was collected by filtration, and washed with ethanol (5 × 2 mL). For recrystallization, the compound was dissolved in hot water (ca. 40 °C) and kept at 4 °C for several days to get a green crystalline compound along with some X-ray diffraction quality crystals. The product was collected by filtration, washed with ethanol (4 × 10 mL), and dried over fused $CaCl_2$. Yield: 0.24 g (45%). Anal. Calcd. for $C_{13}H_{28}NiN_4O_{12}S$: C, 29.84; H, 5.36; N, 10.71. Found: C, 29.41; H, 5.07; N, 10.87. IR (KBr disk, cm^{-1}): ν(O−H), 3575s; ν(N−H), 3250b; ν(C═N) 1656s; ν(C−O/phenolate), 1548s; $\nu(SO_4)$, 1107s, and 620s; $\nu(C-NO_2)$, 844m. $\mu_{eff} = 3.33\ \mu_B$ at 25 °C.

$[Ni(L^3\text{-}O)](BPh_4)$ (3). A solution of $Ni(ClO_4)_2\cdot 6H_2O$ (0.36 g, 1 mmol) in methanol (20 mL) was added dropwise to a stirred solution of the ligand L^3-OH (0.31 g, 1 mmol), also taken in methanol (10 mL). The resultant red solution was refluxed for 1 h. Sodium tetraphenylborate (0.5 g) in solid was then added to this hot solution and filtered. The filtrate was kept at room temperature for several days to obtain an orange microcrystalline compound. It was collected by filtration, washed with Et_2O (2 × 5 mL), and finally dried in a vacuum. The compound was recrystallized from an acetone/petroleum ether (60−80 °C) mixture. X-ray diffraction grade crystals were obtained by diffusing *n*-hexane into an acetone solution of the compound. Yield: 0.38 g (55%). Anal. Calcd for $C_{37}H_{37}BrNiN_3O$: C, 64.50; H, 5.37; N, 6.10. Found: C, 64.10; H, 5.41; N, 6.10. IR (KBr disk, cm^{-1}): ν(N−H), 3281s; ν(C═N), 1623s; ν(C−O/phenolate), 1527s; $\nu(BPh_4)$, 735s, and 707s.

Physical Measurements. Room-temperature magnetic moments, UV−vis spectra, and IR spectra (as KBr disk) were obtained as described elsewhere.[22,23] ^{1}H NMR measurements were performed with a Bruker Model Avance DPX 300 apparatus. Elemental analyses (for C, H, and N) were performed in this laboratory (at IACS) using a Perkin-Elmer 2400 analyzer.

X-ray Crystallography. Selected crystallographic data are given in Table 1, and complete data are given in the supplementary CIF file (see Supporting Information). Intensity data for **1a** were collected at room temperature on a Bruker 1K SMART CCD diffractometer using $\theta-2\theta$ technique, while for **1b**, **2**, and **3** data were collected on a Nonius Kappa CCD diffractometer, with both diffractometers using Mo Kα X-radiation ($\lambda = 0.710\ 73$ Å). No crystal decay was observed during the data collections. The analyzed crystals of **1b**, **2**, and **3** were covered with a thin layer of light oil and cooled at 110 K in order to minimize structural disorder and thermal motion effect and to increase the precision of the results. Intensity data for all the complexes were measured within the θ range of 2.42−27.90°. The structures were solved by direct and Patterson methods and refined by a full matrix least-squares procedure based on F^2 using the SHELXS-97 (**1a**), SIR-92 (**1b** and **2**), DIRDIF-96 (**3**), and SHELXL-97 software.[24−26]

Variable Temperature Magnetic Susceptibility Measurements. The octahedral−square-planar equilibrium of **1a**−**1b** in solution was monitored by susceptibility (χ_g) measurement at variable temperatures following Evans's method.[27] The working solution in D_2O containing 2% *tert*-butyl alcohol as a reference compound was prepared by dissolving 0.0427 g of **1b** per milliliter of the solvent. The solution was taken in a NMR tube. The same combination of solvent (2% *tert*-butyl alcohol in D_2O) was also used as external standard and taken in a capillary tube of 2 mm outer diameter. The latter was placed inside the NMR tube, and the combination was used for Δf measurements in the temperature

(22) Dutta, S. K.; Kumar, S. B.; Bhattacharyya, S.; Tiekink, E. R. T.; Chaudhury, M. *Inorg. Chem.* **1997**, *36*, 4954.
(23) Dutta, S. K.; McConville, D. B.; Youngs, W. J.; Chaudhury, M. *Inorg. Chem.* **1997**, *36*, 2517.
(24) Sheldrick, G. M. *SHELX-97: Programs for Crystal Structure Analysis*, Release 97-2; University of Göttingen: Göttingen, Germany, 1998 (includes SHELXS-97 and SHELXL-97).
(25) Altomare, A.; Cascarano, G.; Giacovazzo, C.; Guagliardi, A.; Burla, M. C.; Polidori, G.; Camalli, M. SIR-92; *J. Appl. Crystallogr.* **1994**, *27*, 435.
(26) Beurskens, P. T.; Admiraal, G.; Beurskens, G.; Bosman, W. P.; Garcia-Granda, S.; Gould, R. O.; Smits, J. M. M.; Smykalla, C. *The DIRDIF-96 Program System*; Technical Report of the Crystallography Laboratory; University of Nijmegen: Nijmegen, The Netherlands, 1996.
(27) Evans, D. F. *J. Chem. Soc.* **1959**, 2003.

range 298−338 K, using a Bruker DPX 300 NMR spectrometer, operated at 300 MHz frequency. The spectral width was 7.5 ppm (2269 Hz), and for each spectrum, 300 scans were recorded.

The ^{1}H NMR spectra of the reference compound in the two coaxial tubes, due to the difference in their volume susceptibilities, exhibit chemical-shift differences (Δf), which are measured (in hertz) and used to calculate the mass susceptibility (χ_g) of the dissolved paramagnetic molecule from

$$\chi_g = \frac{3\Delta f}{2\pi f m} + \chi_o + \frac{\chi_o(d_o - d_s)}{m} \quad (1)$$

where f is the operating radio frequency (in hertz) of the spectrometer, m is the concentration of the paramagnetic substance in grams per milliliter, and χ_o is the mass susceptibility of the pure solvent; d_o and d_s are the densities of the pure solvent and the solution, respectively. The last term in eq 1 can be neglected in all calculations (as it would introduce an error much less than 1%), the details of which are described elsewhere.[28]

Results and Discussion

Synthesis. Three new ligands (L^1-OH−L^3-OH) have been prepared by Schiff base condensation between 1-(2-aminoethyl)piperazine and salicylaldehyde or its 5-substituted nitro and bromo derivatives. The conformational flexibility of the piperazine ring (from boat to chair form and vice versa) makes one of these ligands (L^1-OH) capable of coordinating in ambidentate fashion, generating interesting chemistry of Ni(II) ion in solution as well as in the solid state. Thus with the ligand L^1-OH the complex formation process is very much dependent on the counteranion. The solution appears to be green at room temperature in the presence of Cl^- and SO_4^{2-} ions, while with ClO_4^-, Br^-, and BPh_4^- anions the solutions are yellow to orange in color. We have been successful in isolating the red compound **1a** in the solid state as a tetraphenylborate salt from a boiling methanolic solution. The corresponding green compound **1b** could be obtained in the solid state only in the presence of sulfate anion by cooling at subambient temperature. With the nitro derivative ligand L^2-OH, however, the only product obtained is the green crystalline compound **2**, which in solution can withstand temperatures up to 100 °C without showing any change in color. The latter compound, like **1b**, has been isolated in the solid state only in the presence of sulfate anion. With the bromo derivative ligand L^3-OH, the exclusive product is a red crystalline compound **3**, isolated only as BPh_4 salt as in the case of **1a**, which shows only a marginal color change on cooling at ca. 77 K. The presence of other anions has no effect on the compositions of **2** and **3**, nor do the anions have any impact on the isolation of these compounds.

The sterically constrained ligand L^1-OH plays an interesting role in the formation of **1a** and **1b**, with the former being a diamagnetic square-planar compound while the latter is a paramagnetic ($\mu_{eff} = 3.32\ \mu_B$) octahedral one. As revealed from X-ray crystallographic analysis (see below), the ligand L^1-OH is tetradentate in **1a** with two of its four donor atoms being contributed by the nitrogen atoms of the piperazine moiety in boat conformation. In **1b**, on the other hand, the ligand is tridentate with piperazine moiety in chair conformation, making only a single ring nitrogen atom available for coordination to the nickel center, while the other in the protonated form stays away from coordination. The remaining coordination sites in **1b** are taken up by three water molecules. The overall composition of **1b** is $[Ni(L^1\text{-NH})(H_2O)_3](SO_4)\cdot 6H_2O$, in which L^1-NH stands for the N-protonated form of the ligand L^1-OH.[20] Compounds **2** and **3** have geometry and coordination environments closely similar to those of **1b** and **1a**, respectively.

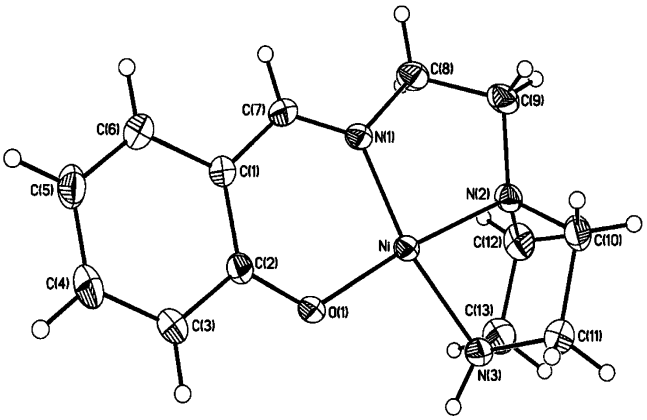

Figure 1. Molecular structure of complex **1a** showing the atom numbering scheme.

IR spectra of the complexes have a couple of prominent bands appearing at ca. 1640 and 1535 cm^{-1} regions, assignable to ν(C═N) and ν(C−O/phenolate) stretching modes, respectively. In the high-frequency region, a broad medium intensity band in the 3500−3400 cm^{-1} range due to ν(O−H) vibration indicates the presence of coordinated water molecules in **1b** and **2**. Compounds **1a** and **3**, on the other hand, show a strong sharp band due to ν(N−H) stretching at ca. 3270 cm^{-1}. In addition, the octahedral complexes **1b** and **2** display two strong bands at 1100 and 620 cm^{-1}, confirming the presence of ionic sulfate.[29] Likewise, **1a** and **3** show two strong bands at ca. 710 and 610 cm^{-1} due to phenyl ring vibrations, associated with tetraphenylborate anion.

Description of Crystal Structures. Figures 1 and 2 show the perspective views of the square-planar complexes of **1a** and **3**, respectively. Their selected bond distances and angles are given in Table 2. Complex **1a** crystallizes in the triclinic space group $P\bar{1}$ with two molecules per unit cell, while **3** has the hexagonal space group $P6_5$ with six molecules in the unit cell. The observed crystal structures confirm the boat conformation of the associated piperazine ring in the ligands. The latter binds to Ni(II) in tetradentate fashion, providing an N_3O donor set. In both molecules, the Ni−N bond distances are slightly different, with the piperazine associated Ni−N(3) bond being the longest: 1.931(2) Å in **1a** and 1.915(6) Å in **3**. The trans angles O(1)−Ni−N(2) and N(1)−Ni−N(3) in **1a** are 172.88(7)° and 163.79(7)°, respectively. Corresponding angles in **3** are almost identical (Table 2). The two halves of the molecule (Ni, O(1), and N(1)) and

(28) Crawford, T. H.; Swanson, J. *J. Chem. Educ.* **1971**, *48*, 382.

(29) Nakamoto, K. *Infrared and Raman Spectra of Inorganic and Coordination Compunds*, 3rd ed.; Wiley-Interscience: New York, 1978.

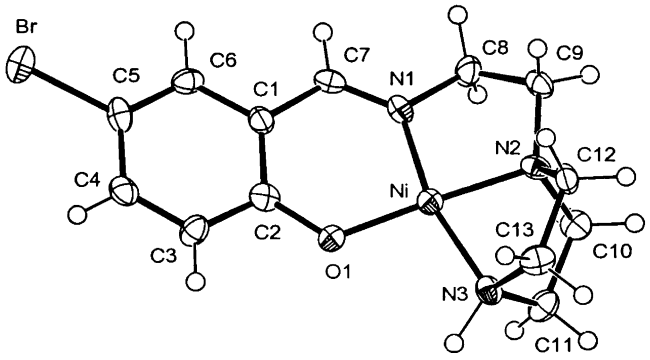

Figure 2. Molecular structure of complex **3** showing the atom numbering scheme. The atomic displacement parameters of the non-hydrogen atoms are represented by 50% probability thermal ellipsoids (darkened for non-C atoms).

Table 2. Selected Bond Lengths (Å) and Angles (deg) for Complexes **1a** and **3**

	1a	**3**
	(a) Bond Lengths	
Ni−O(1)	1.8148(14)	1.798(5)
Ni−N(1)	1.8232(16)	1.836(6)
Ni−N(2)	1.8738(16)	1.888(6)
Ni−N(3)	1.9312(17)	1.915(6)
	(b) Bond Angles	
O(1)−Ni−N(1)	97.21(7)	96.8(2)
O(1)−Ni−N(2)	172.88((7)	173.8(3)
O(1)−Ni−N(3)	98.00(7)	98.7(2)
N(1)−Ni−N(2)	88.62(7)	87.8(3)
N(1)−Ni−N(3)	163.79(7)	163.9(3)
N(2)−Ni−N(3)	76.65(8)	77.0(3)

(Ni, N(2), and N(3)) are twisted by 7.9° in **1a**. The corresponding angle for **3** is 6.8°.

The molecular structures and atom numbering schemes for the cations in the complexes **1b** and **2** are shown in Figures 3 and 4, respectively, and the selected geometric parameters are listed in Table 3. Both complexes crystallize in triclinic space group $P\bar{1}$ and have two molecular units accommodated in the unit cell. Unlike in **1a** and **3**, the ligands here behave in a tridentate fashion due to a conformational change (from boat to chair form) of the associated piperazine ring, generating distorted octahedral structures for **1b** and **2** (Figures 3 and 4). Three atoms O(1), N(1), and N(2) from the tridentate ligand, along with an oxygen atom O(3) from a coordinated water molecule, occupy the meridian plane, while the apical positions are taken up by two other oxygen atoms O(2) and O(4) also coming from the coordinated water molecules. The trans angles O(1)−Ni−N(2), 173.36(6)° (170.77(5)° for **2**); N(1)−Ni−O(3), 175.45(6)° (176.85(5)°); and O(2)−Ni−O(4), 176.34(6)° (172.94(4)°), are close to linearity. The Ni atom lies essentially in the meridian plane, being formally displaced by 0.01 Å (0.02 Å) from the least-squares plane of O(1), N(1), N(2), and O(3), toward the apical oxygen atom O(2).

Of particular interest in the octahedral complexes is the zwitterionic nature of the tridentate ligands arising from the protonation of the N(3) piperazine ring atom, which stays away from coordination due to the chair conformation of the ring. The overall electroneutrality of the coordinated tridentate ligands generates cationic nickel(II) complexes that require sulfate anion for their crystallization. There are six and two water molecules present in **1b** and **2**, respectively, as crystallization solvent. Extensive hydrogen bonding among these and coordinated water molecules, the sulfate ion, and the N−H protons of the piperazinium ring play a significant role in the stabilization of the octahedral products leading

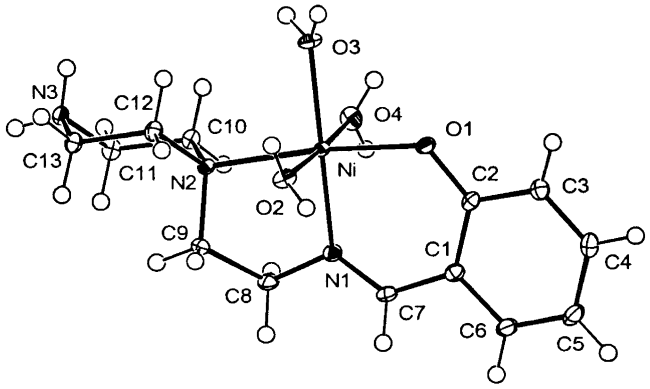

Figure 3. ORTEP drawing and crystallographic numbering scheme for complex **1b**. The atomic displacement parameters of the non-hydrogen atoms are represented by 50% probability thermal ellipsoids (darkened for non-C atoms).

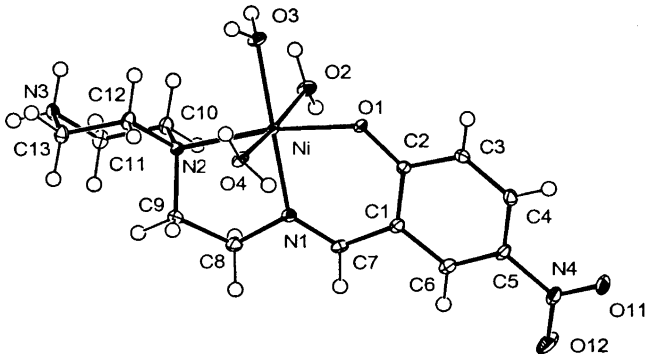

Figure 4. ORTEP drawing and crystallographic numbering scheme for complex **2**. The atomic displacement parameters of the non-hydrogen atoms are represented by 50% probability thermal ellipsoids (darkened for non-C atoms).

Table 3. Selected Bond Lengths (Å) and Angles (deg) for Complexes **1b** and **2**

	1b	**2**
	(a) Bond Lengths	
Ni−O(1)	2.0232(15)	2.0295(13)
Ni−N(1)	1.9997(16)	2.0080(13)
Ni−N(2)	2.2321(16)	2.2153(15)
Ni−O(2)	2.0844(13)	2.0863(12)
Ni−O(3)	2.0534(14)	2.0912(12)
Ni−O(4)	2.0915(14)	2.0566(11)
	(b) Bond Angles	
O(1)−Ni−N(1)	91.57(6)	90.08(5)
O(1)−Ni−N(2)	173.36(6)	170.77(5)
N(1)−Ni−N(2)	82.72(6)	82.49(6)
O(1)−Ni−O(2)	89.99(6)	89.17(5)
O(1)−Ni−O(3)	90.02(6)	88.49(5)
O(1)−Ni−O(4)	93.56(6)	90.60(5)
N(1)−Ni−O(2)	91.01(6)	93.55(5)
N(1)−Ni−O(3)	175.45(6)	176.85(5)
N(1)−Ni−O(4)	89.78(6)	93.11(5)
N(2)−Ni−O(2)	86.75(6)	96.71(5)
N(2)−Ni−O(3)	95.93(6)	97.12(5)
N(2)−Ni−O(4)	89.81(6)	86.47(5)
O(2)−Ni−O(3)	93.25(5)	83.39(5)
O(2)−Ni−O(4)	176.34(6)	172.94(4)
O(3)−Ni−O(4)	85.36(6)	89.98(5)

Table 4. Hydrogen Bonding Parameters for Compounds **1b** and **2**

A	H	B	A···B	A−H	H···B	A−H···B
			1b[a]			
O10	H2#	O6	2.873(2)	0.8547	2.0413	164.08
O11	H3#	O6	2.759(2)	0.8081	1.9744	163.63
O13	H8#	O5	2.810(2)	0.7960	2.0615	154.54
N3	H83A	O5	2.816(2)	0.9000	1.9637	157.48
O14	H14B	O8	2.895(2)	0.8979	2.0009	173.59
N3	H83B	O7	2.788(2)	0.8868	1.9030	175.41
O4	H94A	O8	2.717(2)	0.8289	1.9366	156.53
O4	H94B	O5	2.784((2)	0.8653	1.9193	178.83
O9	H99A	O7	2.743(2)	0.9245	1.8410	164.51
			2[b]			
N3	H3A	O7	2.698(2)	0.9112	1.7990	168.47
N3	H3B	O7	3.2030(18)	0.9385	2.5846	123.79
N3	H3B	O8	2.7588(17)	0.9385	1.8259	172.23
O10	H90A	O6	2.805(2)	0.8478	1.9578	178.47
O2	H92B	O7	2.6952(17)	0.8618	1.8508	166.06
O3	H93B	O6	2.7107(17)	0.9064	1.8053	176.68
O4	H94A	O8	2.6874(19)	0.8328	1.8599	172.22
O9	H99A	O5	2.7402(19)	0.8628	1.8786	176.48

[a] O2−O4 represent water molecules coordinated to the Ni cation, O5−O8 are part of the SO_4 anion, and O9−O14 represent other free water molecules incorporated into the crystal lattice. [b] O9 and O10 represent free water molecules incorporated into the crystal lattice.

Table 5. Summary of Electronic Spectral Data in Solution

complex	solvent	λ_{max}/nm (ϵ_{max}/mol^{-1} cm^2)
1a	CH_3CN	286 (38 900), 318 (12 100), 384 (4450), 451 (sh)
1b	H_2O	233 (19 100), 264 (7850), 354 (5950), 617 (7), 746 (5), 944 (15)
2	H_2O	230 (17 550), 247 (12 200), 384 (14 600), 610 (10), 746 (8), 938 (18)
3	CH_3CN	239 (25 900), 313 (4450), 396 (3250), 466 (sh)

to their crystallization. Details of the hydrogen bonding parameters are listed in Table 4, while Figure S1 (in the Supporting Information) provides a complete view of the atoms participating in hydrogen bonding in **1b**. In the octahedral complexes, the Ni−O and Ni−N distances are in the ranges 2.0232(15)−2.0915(14) and 1.9997(16)−2.2321(16) Å, respectively, which are as expected for high-spin Ni(II) complexes reported so far.[30,31] When these distances are compared with the corresponding bond lengths of the square-planar complexes, an interesting correlation emerges between the structural features of **1a** and **1b**. The bond lengths in **1b** are systematically larger compared to the corresponding distances in **1a**. This is, however, not unexpected[32] considering in the high-spin complex **1b** the presence of a singly populated $d_{x^2-y^2}$ orbital, which is antibonding in nature. This, in consequence, results in an expansion of the basal core, leading to longer bond distances in **1b** compared to the square-planar analogue **1a**.

Electronic Spectra. Electronic spectral data for the complexes are summarized in Table 5. In acetonitrile, **1a** displays a medium intensity band at 451 nm (λ_{max}, for the corresponding band in **3** is 466 nm) in the form of a shoulder due to the spin-allowed $^1A_{1g} \rightarrow {}^1A_{2g}$ transition, typical of square-planar d^8 species.[33] The second ligand-field band, $^1A_{1g} \rightarrow {}^1B_{1g}$, expected to appear at higher energy is probably obscured by the tail of a near-UV absorption present in **1a** and **3**.

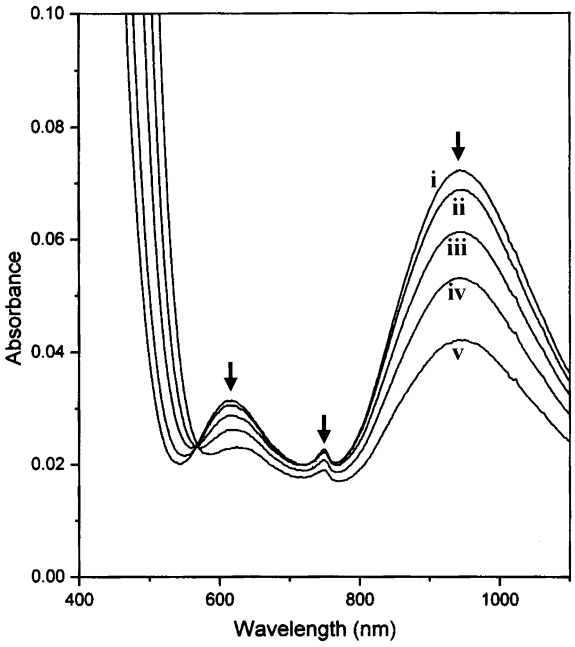

Figure 5. Electronic absorption spectra of **1b** (concentration 4.7×10^{-3} M) in aqueous solution as a function of temperature: (i) 298, (ii) 308, (iii) 318, (iv) 328, and (v) 338 K.

The green octahedral complexes **1b** and **2**, isolated as their sulfate salts, are only soluble in water. In the visible region, aqueous solutions of these complexes display three weak band maxima (ϵ, 5−18 mol^{-1} cm^2) at 944 (938 for **2**), 746 (746), and 617 nm (610 nm) (Figure 5i) corresponding to the spin-allowed transitions $^3A_{2g} \rightarrow {}^3T_{2g}$, $^3A_{2g} \rightarrow {}^3T_{1g}$, and $^3A_{2g} \rightarrow {}^3T_{1g}(P)$, respectively, as expected for Ni(II) in a distorted octahedral environment.[33]

When the temperature of an aqueous solution of **1b** is slowly increased, its color gradually changes from green to light orange with a concomitant change in spectral intensity. In the visible region, all the d−d bands show a decrease in spectral intensities with the rise in temperature as shown in Figure 5. The appearance of isobestic points at 568 nm is a clear indication of the existence of an equilibrium in solution between the octahedral species **1b** and its square-planar counterpart **1a** formed at higher temperatures (vide supra) and is represented by eq 2.

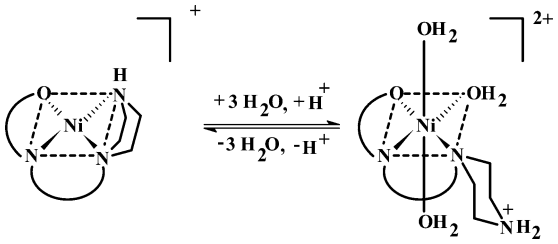

(2)

Equilibrium Studies. Since one component of this equilibrium is a paramagnetic species while the other is a

(30) Jeffery, J. C.; Ward, M. D. *J. Chem. Soc., Dalton Trans.* **1992**, 2119.
(31) Psomas, G.; Stemmler, A. J.; Dendrinou-Samara, C.; Bodwin, J. J.; Schneider, M.; Alexiou, M.; Kampf, J. W.; Kessissoglou, D. P.; Pecoraro, V. L. *Inorg. Chem.* **2001**, *40*, 1562.
(32) (a) Duval, H.; Bulach, V.; Fischer, J.; Weiss, R. *Inorg. Chem.* **1999**, *38*, 5495. (b) Fabbrizzi, L.; Micheloni, M.; Paoletti, P. *J. Chem. Soc., Dalton Trans.* **1980**, 134.
(33) Lever, A. B. P. *Inorganic Electronic Spectroscopy*, 2nd ed.; Elsevier Science: Amsterdam, 1984.

Table 6. Magnetic and Equilibrium Data for the Planar ⇌ Octahedral Equilibrium in Aqueous Solution Involving **1a** and **1b**

temp (K)	μ	% planar	% octahedral	K_{eq}
298	3.18	8.3	91.7	11.04
308	3.09	13.4	86.6	6.46
318	2.93	22.1	77.9	3.52
328	2.72	32.9	67.1	2.04
338	2.51	42.9	57.1	1.33

diamagnetic one, this offers an opportunity[14,28] to follow the above equilibrium by magnetic measurements in solution using ^{1}H NMR technique as proposed by Evans.[27] With an aqueous solution of **1b**, the magnetic moments have been measured in the temperature range 298−338 K following this methodology as summarized in the Experimental Section. A gradual decrease in the magnetic moment value, as displayed in Table 6, with the rise in temperature is a clear indication of the transformation of **1b** into the diamagnetic species **1a**. The percentage of diamagnetic species present in solution has been calculated using[15,28]

$$\% \text{ diamagnetic species} = 100[1 - \mu^2/(3.32)^2] \qquad (3)$$

where μ is the magnetic moment of the solution at any particular temperature and 3.32 μ_B is the magnetic moment of pure **1b** in the solid state.

The equilibrium constant K_{eq} for eq 2 is defined as K_{eq} = [octahedral]/[planar]. Since eq 2 is pH dependent, K_{eq} here is a composite parameter that includes the contribution due to temperature dependence of pH. The percentage of the planar species increases from 8.3 at 298 K to 42.9 at 338 K with K_{eq} = 11.04 and 1.33 at the above two temperatures, respectively. A plot of log K_{eq} versus 1/T is linear (Figure 6), giving $\Delta H° = -46 \pm 0.2$ kJ mol^{-1} from the least-squares slope (correlation coefficient 0.999 58). The values of $\Delta S°$ obtained at each temperature from the equation $\Delta G° = \Delta H° - T\Delta S°$ give an average value of -133 ± 5 J K^{-1} mol^{-1}. However, the sizes of these thermodynamic parameters appear questionable considering the composite nature of the equilibrium constants.

Concluding Remarks

Structural and equilibrium studies of nickel(II) complexes of flexidentate salicylaldimino Schiff base ligands (L^1-OH−L^3-OH) have been reported here. The piperazinyl arm of these ligands can in principle have either a boat or a chair conformation, leading to square-planar or octahedral geometry, respectively, of the reported complexes. Both remote substitution in the ligand aromatic ring and the nature of the

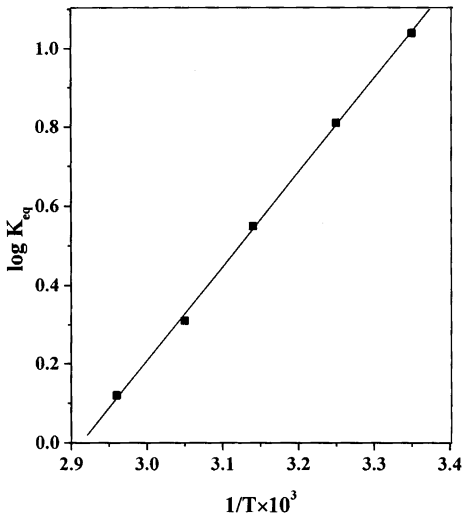

Figure 6. Plot of log K_{eq} versus 1/T for the octahedron−square-planar equilibrium in aqueous solution of Ni(II)−L^1-OH complex.

associated anions have profound influences on the coordination geometry of the complexes. With the ligand L^1-OH, both square-planar (**1a**) and the octahedral (**1b**) complexes have been isolated and crystallographically characterized. In solution, these compounds are in equilibrium (eq 2), which is unique in the sense that both solvation and the change of ligand denticity are simultaneously in operation here. All the other equilibria involving square-planar and octahedral nickel(II) complexes reported so far[5−16] are either due to solvation[5−14] or due to change in ligand denticity.[15,16] Also, unlike the previous examples,[15,16] the ligand denticity here increases as we go up the temperature scale when the octahedral species (**1b**) is gradually converted to the square-planar one (**1a**). Also, this is one of the rare examples[4,12] where both forms involved in equilibrium have been isolated in the solid state and characterized crystallographically.

Acknowledgment. Financial support received from the Council of Scientific and Industrial Research (CSIR), New Delhi, is gratefully acknowledged. Two of us (D.M. and D.G.) thank CSIR for the award of research fellowships. We also thank Professor R. J. Butcher and Dr. Gautom K. Patra for their help in the crystal structure determination of **1a** and **1b**, respectively.

Supporting Information Available: Figure S1; X-ray crystallographic files in CIF format for compounds **1a**, **1b**, **2**, and **3**. This material is available free of charge via the Internet at http://pubs.acs.org.

IC0346174